

EVALUATING OTFS MODULATION FOR 6G: IMPACT OF HIGH MOBILITY AND ENVIRONMENTAL NOISE

Abderrahim Mohammadi ¹, Aziz Dkiouak ², Mostafa Baghour ³, Saad Chakkor ⁴,
Ahmed EL Oualkadi ¹ and Anass El Mamouni ⁴

¹ Laboratory of Innovative System Engineering ENSA of Tetuan, Abdelmalek Essaadi
University Tetuan, Morocco

² STIC Laboratory, Faculty of Sciences, Chouaib Doukkali University, El jadida,
Morocco

³ Smart Materials and Artificial intelligence Team, LCCPS, ENSAM of Casablanca,
University of Hassan II, Morocco

⁴ Laboratory of Information and Communication Technologies (LabTIC) National
School of Applied Sciences of Tangier (ENSATg), Abdelmalek Essaadi University
Tetuan, Morocco

ABSTRACT

Orthogonal Time-frequency-space (OTFS) modulation represents a pioneering advancement tailored to the requirements of prospective sixth-generation (6G) wireless networks. The innovative design effectively addresses the challenges associated with high-frequency dispersion in wireless transmission environments, offering many advantages over traditional modulation schemes such as orthogonal frequency-division multiplexing (OFDM). OTFS stands out due to its capacity to adapt to dynamic wireless channels with high Delay-Doppler (DD) dispersion, a capability that is not present in traditional frameworks. In contrast to conventional approaches, which assume near-channel stability over an OTFS frame, OTFS modulation is well-suited to environments where the input-output relationship may vary over time due to evolving media or environmental conditions. In a comparative analysis with OFDM, OTFS exhibits superior block error rate (BLER) performance compared to the signal-to-noise ratio (SNR) across varying modulation formats, including QPSK, 16QAM, and 64QAM. Numerical simulations demonstrate that OTFS outperforms OFDM in mitigating transmission errors in diverse scenarios by exploring different reception rates for each waveform.

KEYWORDS

6G, DD, OTFS, OFDM, BLER, SNR.

1. INTRODUCTION

Over the past ten years, networks have transmitted exabytes of data, fueled by advancements in autonomous vehicles, extensive sensor networks, the Internet of Things (IoT), and the early development of immersive media. This has resulted in the creation of billions of new connected endpoints with varying sensitivities and Quality of Service (QoS) demands, highlighting several deficiencies in current network technologies. To address these challenges, the International Telecommunication Union (ITU) established the Network 2030 Think Tank in mid-2018, aiming to explore future system technologies for 2030 and beyond. The paper [1] focuses on meeting the communication needs of society by 2030 and identifying the network technologies required

to provide high-resolution immersive services multimedia over IoT, factory automation, and self-driving cars to become a reality.

The current wireless communication systems, such as 4G and 5G, struggle to meet the stringent demands for high data rates, low latency, and reliable performance under high mobility conditions. Orthogonal Frequency Division Multiplexing (OFDM) has been the prevalent technology in these systems, offering near-capacity performance in linear time-invariant channels and mitigating inter-symbol interference (ISI) caused by time dispersion. However, OFDM's performance heavily depends on maintaining orthogonality between subcarriers, which can be compromised by Doppler shifts, leading to significant intercarrier interference (ICI) [2]. Furthermore, emerging applications like vehicle-to-vehicle (V2V) communications, the Internet of Things (IoT), and Industry 4.0 demand new wireless communication systems that can perform reliably in high-mobility environments [3]. Thus, the existing OFDM modulation may not suffice for efficient and dependable communications in these scenarios [4].

To satisfy the diverse requirements of the impending 6G networks, the recently suggested Orthogonal Time Frequency Space (OTFS) modulation has attracted a lot of interest [5]. OTFS processes signals in the Doppler-delay domain, simplifying receiver design and effectively managing Doppler effects encountered in high-speed situations. Unlike OFDM, OTFS can function with fewer pilot signals, and its symbol detection is less complex [6]. This method enables the efficient and adaptable arrangement of reference signals by transforming the fluctuating channel over time into a stable channel in the delay-Doppler domain, which has two dimensions. Additionally, OTFS modulation provides enhanced robustness to high mobility scenarios, making it a promising candidate for next-generation wireless communication [7].

The article has been structured as below. Section II provides a mathematical analysis of the modulation and demodulation of OTFS systems for transmitter and receiver in the presence of delay and Doppler effects. In Section III, we analyze the bit-error-rate performance of OTFS systems compared with OFDM systems based on numerical results. First, we study the variation of BLER versus SNR for the different bit per symbol (QPSK, 16QAM, 64QAM) for a fixed and mobile receiver at five speeds, 0kmph, 100kmph, 160 kmph, 200kmph, and 320 kmph. Next, we will compare the BLER of the two modulation schemes versus SNR. Then by comparing the two systems OTFS and OFDM in terms of BLER for two numbers of subcarriers $M=128$ and 512 in the case of a speed of 320Kmph with QPSK 16QAM.

Notating: Scalars, vectors, and matrices are written in normal, small, and large capitals, respectively. The symbols $(\cdot)^T$ and $(\cdot)^H$ used to designate the operations of transposition and conjugate transposition, respectively. In mathematics, the imaginary number j is defined as the square of the negative one, i.e., $j^2 = -1$. A matrix, A matrix called $A = [a_{nm}]_{N \times M}$ has N rows and M columns with each element a_{nm} is characterized as belonging to the set \mathcal{C} and placed in the n -th row and m -th column of A . $A \otimes B$ is the Kronecker product of the matrices A and B . Also, $\mathbf{a} = [a_n]_{N \times 1}$ represents a vector comprising a column, with $a_n \in \mathcal{C}$ this is in the n -th row of \mathbf{a} . The $\text{vec}(\mathbf{A})$ operator creates a $NM \times 1$ column vector, where the columns in the $N \times M$ matrix \mathbf{A} are stacked. The N -point discrete Fourier transform (DFT) matrix is given in the following form

$$\mathbf{F}_N = \frac{1}{\sqrt{N}} [e^{-j^2 2\pi \frac{kn}{N}}]_{N \times N}$$

where $\mathbf{F}_N \mathbf{F}_N^H = \mathbf{I}_N$ with \mathbf{I}_N representing the identity matrix. [8]

2. RELATED WORK

OTFS stands out as a strong candidate for 6G networks due to its superior resilience to Doppler effects, making it ideal for high-mobility scenarios such as vehicular and satellite communications. Unlike OFDM and other multicarrier techniques like GFDM, FBMC, and UFMC, OTFS spreads symbols across both time and frequency domains, achieving full diversity gain and improving link reliability in fading channels. It also offers higher spectral efficiency by eliminating cyclic prefix overhead while maintaining low pilot overhead for channel estimation, reducing complexity in massive MIMO systems. Additionally, OTFS enables seamless integration with existing OFDM-based networks, ensuring backward compatibility for an efficient transition to 6G. While OTFS has higher computational complexity, its benefits in robustness, interference management, and adaptability to dynamic environments justify its feasibility for future wireless communication systems.

Recent studies have highlighted the advantages of Orthogonal Time Frequency Space (OTFS) modulation over traditional schemes like Orthogonal Frequency Division Multiplexing (OFDM) and other multicarrier techniques in the context of 6G networks. A study published in 2023 emphasizes OTFS's robustness in high-mobility scenarios, noting its superior resilience to Doppler effects compared to OFDM [9]. Additionally, OTFS has been recognized for its improved energy efficiency in dynamic environments, which is crucial for the energy demands of future 6G applications [10]. Furthermore, OTFS's operation in the delay-Doppler domain allows for better handling of time-varying channels, offering significant advantages in high-mobility contexts [11]. These findings underscore OTFS's potential as a key enabler for reliable and efficient communication in next-generation wireless networks.

The extant literature on the subject of OTFS modulation in high-mobility and 6G scenarios is highlighted. Research in [12] introduces channel estimation for doubly dispersive channels, but analysis of high-mobility environments and dynamic adaptation is lacking. Studies such as [13, 14, 15] explore OTFS for delay-Doppler systems, demonstrating its potential for 6G but neglecting trade-offs in complexity and reliability. While [16] provides a strong mathematical framework, it does not address OTFS-OFDM coexistence or interference management in dense networks. Works such as [17] combine OTFS with PDMA for IoT but overlook interference mitigation and mixed mobility scenarios. Enhanced OTFS schemes like [18] and [19] improve performance in time-variant channels but ignore complex real-world models. [20] proposes an efficient OTFS receiver design for high-speed vehicular communication, using large-scale antenna arrays to reduce complexity and overhead. However, it does not address interference management in dense vehicular networks or its impact on QoS. Similarly, [21] introduces an ML-based system to switch between OTFS and OFDM adaptively, optimizing performance based on channel conditions. Yet, it overlooks the computational complexity of ML in real-time systems and lacks discussion on interference management in multi-user or multi-cell environments, which are critical for dense networks. Despite the advantages of OTFS, including full diversity and resilience in high-mobility environments [22, 23], challenges such as inter-symbol interference and high computational complexity remain [24]. Recent studies have focused on modulation and coding techniques [25, 26], but this work aims to address gaps in interference management, integration with legacy systems, and computational efficiency.

3. OTFS SYSTEM

The following section outlines the basic principles of OTFS modulation, which are essential for comprehending the presented research. Specifically, the key functions of the OTFS modulation

system's transmitter and receiver are detailed in the functional diagram in Figure 1. The information is based on the articles [27], [28].

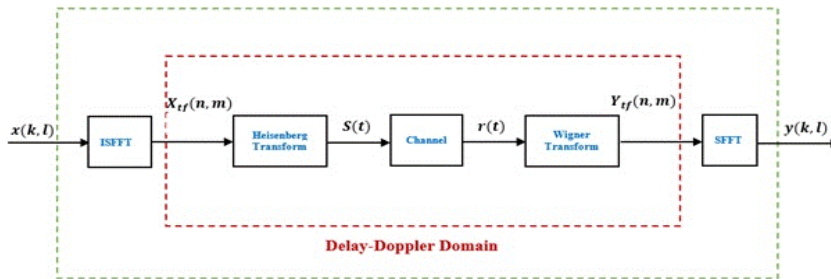


Figure 1: OTFS modulation scheme.

2.1. OTFS Transmitter

OTFS modulation is a two-dimensional technique, that modulating data in the DD domain and then transforms the signals into the TF and time domains. The time-frequency discretization grid with a time axis and a frequency axis in interims $T(s)$ and $\Delta f(Hz)$ is illustrated in Figure 1.

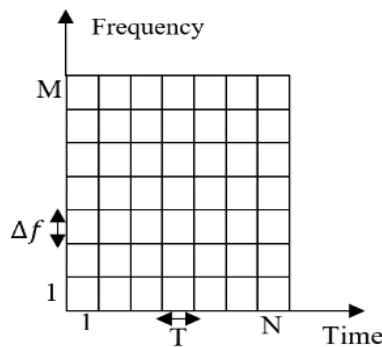


Figure 2: Equivalent grid for the time-frequency domain

From Figure 2, we obtain that the OTFS frame is transmitted within a time $T_{frame} = NT$ and occupies a bandwidth $B_{frame} = M\Delta f$.

Figure 2 defines the delay-Doppler plane:

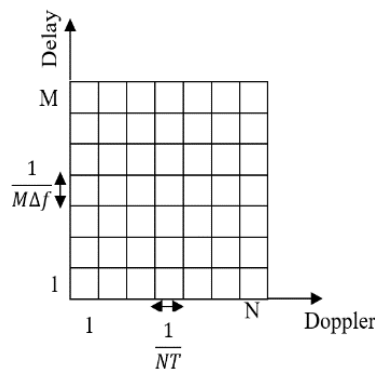


Figure 3: Equivalent grid for delay-Doppler domain

where $\frac{1}{MAf}$ and $\frac{1}{NT}$ represent the Delay and Doppler frequency quantization steps, respectively.

Let be the set of data symbols $NM \{x(k, l), k=0, \dots, N-1, l=0, \dots, M-1\}$ of a numerical modulation of size q , $A = \{a_1, \dots, a_q\}$ (QPSK or QAM symbols), arranged in the delay-Doppler plane.

In the initial step of the OTFS transmission process, the symbols $x(k, l)$ are mapped into NM samples $X_{tf}(n, m)$ on a time-frequency grid using the following ISFFT relation,

$$X_{tf}(n, m) = \frac{1}{\sqrt{NM}} \sum_{k=0}^{N-1} \sum_{m=0}^{M-1} x(k, l) e^{j2\pi(\frac{nk}{N} - \frac{ml}{M})} \quad (1)$$

Where $n=0, \dots, N-1$, $m=0, \dots, M-1$

Subsequently, a time-frequency modulator converts the samples represented by $X_{tf}(n, m)$ into a continuous time waveform, defined by $S(t)$ in the time domain, utilising a transmission waveform denoted by $g_{tx}(t)$. The following relation defines this transformation,

$$S(t) = \sum_{k=0}^{N-1} \sum_{m=0}^{M-1} X_{tf}(n, m) g_{tx}(t-nT) e^{j2\pi m \Delta f (t-nT)} \quad (2)$$

Where, $g_{tx}(t)$ is the pulse of transmitter, Δf is subcarrier spacing and T symbol duration.

An OTFS transmitter can be described by a matrix representation, facilitating software or hardware implementation. It starts with a more condensed form of the ISFFT as shown in Eq 1. We can obtain this equation by the DFT matrices $F_N \in \mathbb{C}^{N \times N}$ and $F_M \in \mathbb{C}^{M \times M}$. If $X^{DD} \in \mathbb{C}^{N \times M}$ includes the symbols $x(k, l)$ representing the DD domain and $X^{TF} \in \mathbb{C}^{N \times M}$ includes the symbols $X_{tf}(n, m)$ of the TF domain.

From the previous notation, we can write Equation 1 in the following matrix form:

$$X^{TF} = F_N^H X^{DD} F_M \quad (3)$$

$$X^{DD} = F_M^H X^{TF} F_N \quad (4)$$

Similarly, we can transform Eq 2 like this.

$$S = X^{TF} F_M^H G_{tx} = (F_N^H X^{DD} F_M) F_M^H G_{tx} = F_N^H X^{DD} G_{tx} \quad (5)$$

In this context, the $G_{tx} \in \mathbb{C}^{M \times M}$ element is responsible for pulse shaping, while the $S \in \mathbb{C}^{N \times M}$ function is dedicated to storing the transmission signals. An alternative approach is to express the transmission signal in the TF domain as a vector.

$$s = \text{vec}(S) = (G_{tx}^T \otimes F_N^H) \text{vec}(X^{DD}) \quad (6)$$

2.2.OTFS Receiver

First, it should be noted that the signal $S(t)$ is transmitted via a channel with a response in the Doppler delay domain, which can be expressed as $h(\tau, \nu)$, with τ and ν representing the delay and Doppler variables, respectively.

The time domain signal, denoted by $r(t)$, is received at the receiver.

$$r(t) = \iint h(\tau, \nu) S(t-\tau) e^{j2\pi\nu(t-\tau)} d\tau d\nu \quad (7)$$

As illustrated below, a Wigner transformation is employed to translate the received signal, $r(t)$, into the time-frequency (TF) domain.

$$Y_{tf}(n, m) = A_{g_{x,y}}(t, f) |_{t=nT, f=m\Delta f} \quad (8)$$

$$A_{g_{x,y}}(t, f) = \int g_{rx}^*(t'-t) y(t) e^{-j2\pi f(t'-t)} dt' \quad (9)$$

In this equation, $g_{rx}(t)$ is the receive pulse shape. If the receive pulse shape $g_{rx}(t)$ and the transmit pulse shape $g_{tx}(t)$ satisfy the bi-orthogonality condition [29], the following equation provides the input-output relation in the time-frequency (TF) domain.

$$Y_{tf}(n, m) = H(n, m) X_{tf}(n, m) + V(n, m) \quad (10)$$

with, $V(n, m)$ representing noise in the time-frequency domain. $H(n, m)$ is defined as follows.

$$H(n, m) = \int_{\tau} \int_{\nu} h(\tau, \nu) e^{j2\pi\nu nT} e^{j2\pi\nu(\nu+m\Delta f)\tau} d\nu d\tau \quad (11)$$

using SFFT the TF signal $Y(n, m)$ is converted into the DD domain signal $y(k, l)$, as follows,

$$y(k, l) = \sum_{n=0}^{N-1} \sum_{m=1}^{M-1} Y_{tf}(n, m) e^{-j2\pi\left(\frac{nk}{N}, \frac{ml}{M}\right)} \quad (12)$$

From the equations above (1)-(7), we can express the input-output relation as follows [20]

$$y(k, l) = \frac{1}{\sqrt{NM}} \sum_{l'=0}^{N-1} \sum_{k'=0}^{M-1} x(k', l') h_w\left(\frac{k-k'}{NT}, \frac{l-l'}{M\Delta f}\right) + v(k, l) \quad (13)$$

The notation $h_w(\nu, \tau)$ represents the circular convolution of the channel response with the windowing function $w(\nu, \tau)$ and

$$h_w\left(\frac{k-k'}{NT}, \frac{l-l'}{M\Delta f}\right) = h_w(\nu, \tau) |_{\nu = \frac{k-k'}{NT}, \tau = \frac{l-l'}{M\Delta f}} \quad (14)$$

In a manner analogous to the transmitter, The OTFS receiver is given by the following matrix expression,

$$Y^{DD} = F_N Y^{TF} F_M^H = F_N (R G_{rx} F_M) F_M^H = F_N R G_{rx} \quad (15)$$

where $R \in \mathbb{C}^{N \times M}$ keeps the signals received, $G_{rx} \in \mathbb{C}^{M \times M}$ indicates the filtering adapted to the pulse shape of the receiver, and Y^{TF} , $Y^{DD} \in \mathbb{C}^{N \times M}$ comprises the received symbols in the TF and DD domains. The signal reception at the DD domain in vector form is expressed as follows

$$y = \text{vec}(Y^{DD}) = (G_{rx}^T \otimes F_N) \text{vec}(R) \quad (16)$$

2.3. Signal-to-Noise Ratio (SNR) in OTFS

The SNR for OTFS in the presence of Gaussian noise is given by:

$$SNR = \frac{E[|H(n, m) \cdot X_{tf}(n, m)|^2]}{E[|V(n, m)|^2]} = \frac{P_{signal}}{\sigma^2} \quad (17)$$

Where P_{signal} is the average signal power.

The noise power σ^2 in the delay-Doppler domain depends on the system's noise spectral density N_0 and the system bandwidth B :

$$\sigma^2 = N_0 \cdot B \quad (18)$$

OTFS modulation spreads symbols across the entire delay-Doppler domain, making the system more resilient to localized noise effects compared to OFDM. However, Gaussian noise in OTFS affects all grid points uniformly in the delay-Doppler domain. The performance is evaluated using metrics such as block error rate (BLER) or signal-to-noise ratio (SNR) [31].

2.4. TDLA Channel model

In [28] The TDLA model incorporates propagation delays and angles of arrival for multipath components, capturing spatial and temporal characteristics. Each multipath component (or tap) is modeled as:

$$h_{TDLA}(t, \tau, \theta) = \sum_{i=1}^N h_i e^{j\phi_i} \delta(\tau - \tau_i) \delta(\theta - \theta_i) \quad (19)$$

N : Total number of taps (multipath components).

h_i : Complex amplitude of the i -th tap, representing the attenuation of the signal.

ϕ_i : Phase of the i -th tap.

τ_i : Delay of the i -th tap, capturing the propagation delay.

θ_i : Angle of arrival (AoA) of the i -th tap.

$\delta(\cdot)$: Dirac delta function, used to represent the specific delay and angular location of each tap.

This representation accounts for the time-domain dispersion τ and the angular domain spread θ , making it suitable for analyzing wireless systems that rely on spatial diversity, such as MIMO systems.

2.5. Performance Indicators

Orthogonal Time Frequency Space (OTFS) modulation introduces additional computational complexity compared to Orthogonal Frequency Division Multiplexing (OFDM) due to its 2D transformations, channel estimation, and equalization processes. Below, we analyze the key contributors to OTFS complexity.

2.5.1. Complexity of ISFFT and SFFT (2D Transformations)

OTFS modulation employs two key transformations:

- a- Inverse Symplectic Finite Fourier Transform (ISFFT) – Converts time-frequency symbols to the delay-Doppler domain.
- b- Symplectic Finite Fourier Transform (SFFT) – Maps delay-Doppler symbols back to the time-frequency domain.

Mathematically, these are represented as expressed in (3) and (4) [31]:

2.5.2. Computational Complexity

Each 1D Discrete Fourier Transform (DFT) operation requires $\mathcal{O}(N\log N)$ or $\mathcal{O}(M\log M)$ operations. Since OTFS requires two 1D transforms (one for ISFFT and another for SFFT), the total complexity is:

$$\mathcal{O}(MN\log M + MN\log N) = \mathcal{O}(MN\log(MN)) \quad (20)$$

This is significantly higher than OFDM, which requires a single $\mathcal{O}(N\log N)$ FFT per symbol [32].

2.5.3. Channel Estimation Complexity

OTFS operates in the delay-Doppler domain, where channel estimation requires handling a 2D sparse channel matrix [33]. The channel response is modeled as:

$$H(\tau, \nu) = \sum_{i=1}^L h_i \delta(\tau - \tau_i) \delta(\nu - \nu_i) \quad (21)$$

where:

- L = Number of multipath components.
- h_i = Channel coefficient for the i^{th} path.
- τ_i, ν_i = Delay and Doppler shift of the i^{th} path.

2.5.4. Computational Complexity of Channel Estimation

- a- Least Squares (LS) Estimation:
- b-

$$\hat{H} = (X^H X)^{-1} X^H Y \quad (22)$$

Complexity: $\mathcal{O}(L^2)$ [34].

- c- Minimum Mean Square Error (MMSE) Estimation:

$$\hat{H} = (X^H X + \sigma^2 I)^{-1} X^H Y \quad (23)$$

Complexity: $\mathcal{O}(L^3)$ due to matrix inversion [35].

OTFS requires more pilot symbols than OFDM for accurate channel estimation in the delay-Doppler domain, further increasing complexity [36].

2.5.5. Equalization Complexity

OTFS uses either MMSE (Minimum Mean Square Error) Equalization or the Message Passing Algorithm (MPA) for symbol detection.

A. MMSE Equalization

$$\hat{X} = (H^H H + \sigma^2 I)^{-1} H^H Y \quad (24)$$

Computational Complexity:

$$\mathcal{O}((MN)^3) \quad (25)$$

Due to matrix inversion, this is highly computationally expensive [37].

B. MPA Equalization

$$P(x) \propto \prod_{i=1}^L P(y_i | x) \quad (26)$$

- Computational Complexity: $\mathcal{O}(MNL)$ (27)
- Lower complexity than MMSE but requires multiple iterations for convergence.

2.5.6. Mathematical Modeling of BLER vs. SNR for OTFS

The Block Error Rate (BLER) in an Orthogonal Time Frequency Space (OTFS) modulation system depends on several factors, including signal-to-noise ratio (SNR), modulation scheme, channel conditions, and receiver equalization techniques. Below is a mathematical formulation of how BLER is modeled in an OTFS system.

For high-mobility conditions, Doppler shifts alter the channel gains, introducing additional SNR degradation. The effective SNR under Doppler spread can be estimated as [38]:

$$\gamma_{\text{eff}} = \frac{\sum_{i=1}^L |h_i|^2}{1 + \frac{f_d T}{M}} \quad (28)$$

where:

- f_d : Maximum Doppler shift is given by $f_d = \frac{v \cdot f_c}{c}$,
- v : Velocity of the receiver (m/s),
- f_c : Carrier frequency (Hz),
- c : Speed of light (m/s),
- T : Symbol duration.

With increased Doppler spread, OTFS leverages delay-Doppler diversity. Thus, a generalized expression for BLER vs. SNR in OTFS can be represented as:

$$BLER \approx 1 - \left(1 - Q \left(\sqrt{\frac{3\gamma_{\text{eff}}}{(M-1)}} \right) \right)^{N \times M} \quad (29)$$

where γ_{eff} is adapted based on Doppler spread, multipath effects, and equalization technique.

4. RESULTS AND DISCUSSIONS

4.1. OTFS and OFDM by varying the speed

4.1.1. Parameters Study

Table 1. Parameters of Simulation

Parameter	value
subcarrier Numbers	64
Carrier frequency (GHz)	2
speed in kmpm	320, 200, 160, 100,0
Subcarrier spacing (KHz)	15
Cyclic Prefix duration (us)	0.67
Channel model	TDLA
MCS	QPSK, 16QAM, 64QAM, rate 0.5

Figure 4 presents a comparative analysis of BLER performance across OTFS and OFDM waveforms for three modulation schemes at a mobility speed of 320 kmph. The BLER versus SNR curves reveal that OTFS outperforms OFDM across all SNR levels for QPSK, 16QAM, and 64QAM modulation schemes. However, the disparity in BLER between OFDM and OTFS for 64QAM is slightly smaller compared to the differences observed for 16QAM and QPSK.

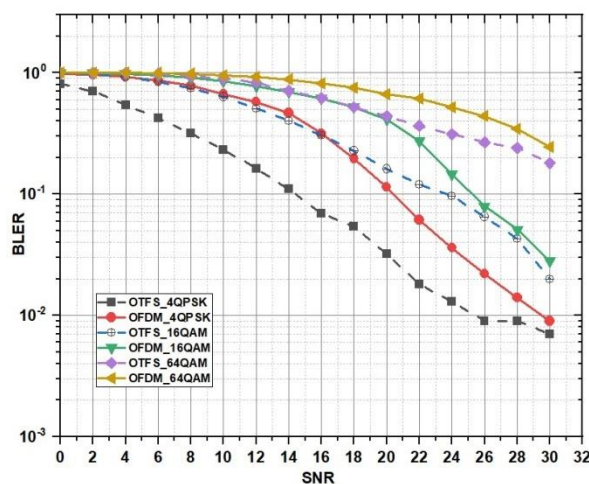


Figure 4: BLER Vs. SNR for OFDM and OTFS (with M=64 subcarriers and velocity 320Km/h) using QPSK, 16QAM, and 64QAM.

Figure 5 compares the BLER of OFDM and OTFS waveforms for various modulation schemes at a mobility velocity of 200 km/h. The BLER is plotted against the SNR to create a curve indicating that OTFS outperforms OFDM at all SNR levels for the QPSK, 16QAM, and 64QAM modulation schemes. However, the BLER mismatch between OFDM and OTFS for 64QAM is slightly smaller than the differences observed for 16QAM and QPSK.

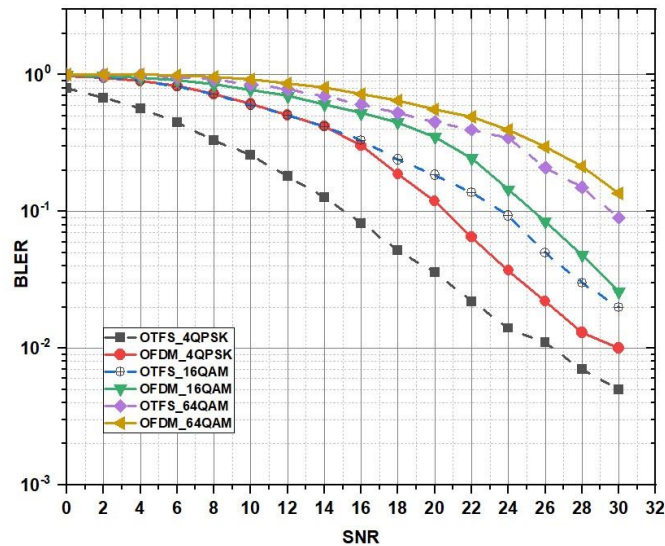


Figure 5: BLER Vs SNR for OFDM and OTFS (using M=64 subcarriers and speed 200Kmph) for QPSK,16QAM, and 64QAM

Figure 6 depicts the BLER comparing the OTFS and OFDM systems for three modulation schemes at a mobility velocity of 160 km/h. The BLER vs. SNR curves demonstrate that OTFS performs better than OFDM across all SNR levels for the QPSK, 16QAM, and 64QAM modulation schemes. Nevertheless, the BLER disparity between OFDM and OTFS for 64QAM is slightly smaller than the differences observed for 16QAM and QPSK.

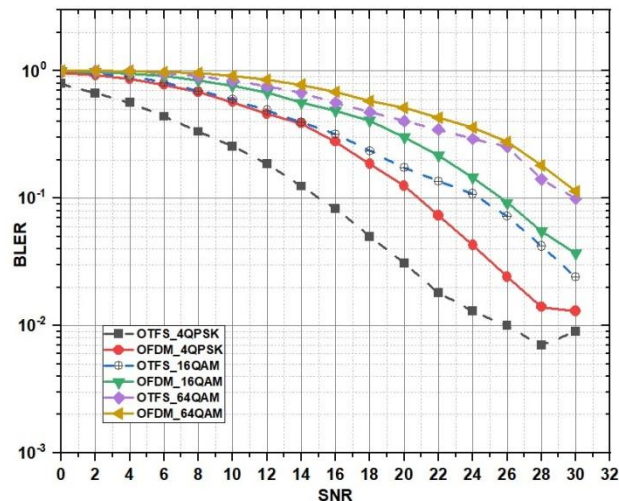


Figure 6: BLER Vs SNR for OFDM and OTFS (using M=64 subcarriers and speed 160Kmph) for QPSK,16QAM, and 64QAM

Figure 7 offers a comparative illustration of the BLER performance achieved by OTFS and OFDM waveforms for three modulation schemes at a mobility speed of 100 km/h. The BLER versus SNR curves indicate that OTFS performs better than OFDM across all SNR levels for the QPSK, 16QAM, and 64QAM modulation schemes. The BLER disparity between OFDM and OTFS for 64QAM, however, is slightly less than the differences observed for 16QAM and QPSK.

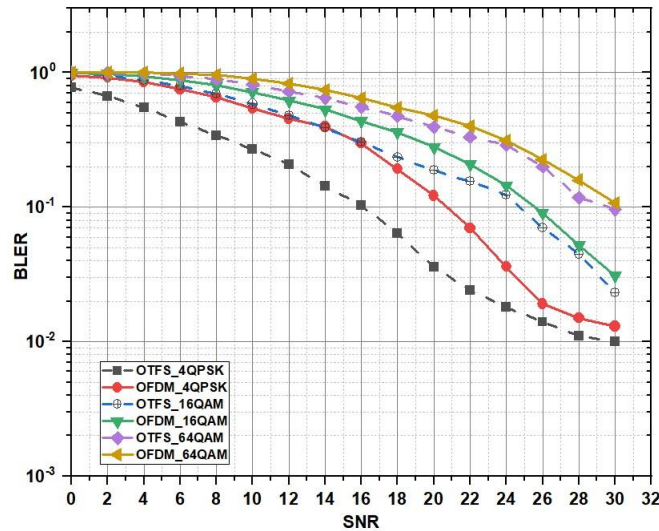


Figure 7: BLER Vs SNR for OFDM and OTFS (using M=64 subcarriers and speed 100Kmph) for QPSK, 16QAM, and 64QAM

Figure 8 indicates a comparative analysis of BLER performed by OTFS and OFDM waveforms for three modulation schemes at a 0 km/h mobility speed. Based on the BLER against SNR curves, OTFS is superior to OFDM at all SNR levels for the QPSK, 16QAM, and 64QAM modulation schemes. The difference in BLER between OFDM and OTFS for 64QAM modulation is, of course, slightly smaller than the differences observed for 16QAM and QPSK modulation.

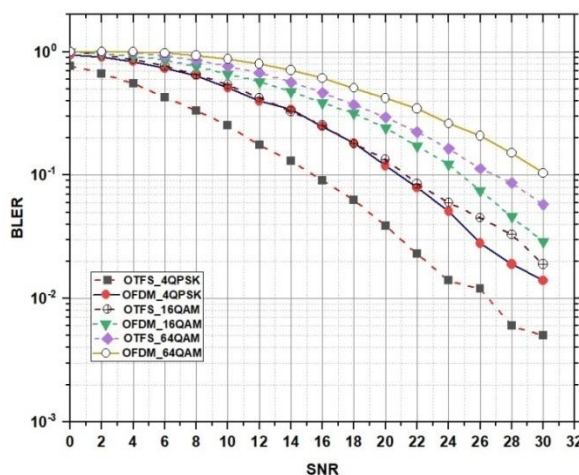


Figure 8: BLER Vs SNR for OFDM and OTFS (M=64 of subcarriers, and velocity 0Kmph) with QPSK, 16QAM and 64QAM

4.1.2. Performance Comparison

As with Figure 4, Figures 5, 6, 7, and 8 plot BLER versus SNR for mobility speeds of 200 km/h, 160 km/h, 100 km/h, and 0 km/h, employing the identical parameters as outlined in Table 1. Figures 5, 6, 7, and 8 illustrate the performance vantage of BLER OTFS over OFDM augments through mobility speed. The findings of Figures 4, 5, 6, 7, and 8 are summarized in Table 2. The data presented in this table demonstrate that the SNR benefit of OTFS over OFDM is amplified with increasing mobility speed, irrespective of the modulation scheme employed.

It is evident that the SNR gain of OFDM with the OTFS scheme, in comparison to OFDM, is amplified with an increasing velocity of mobility for the three distinct modulation schemes. At a BLER of $2 \cdot 10^{-1}$, we find that OTFS has an SNR gain of 7 dB, 6 dB, 5.75 dB, 5.35 dB, and 5.25 dB compared with OFDM, at mobility speeds of 320 km/h, 200 km/h, 160 km/h, 100 km/h and 0 km/h, respectively, for the QPSK modulation scheme. 16QAM SNR gain is equal to 4 dB, 3 dB, 2.75 dB, and 2.25 dB at mobility speeds of 320 km/h, 200 km/h, 160 km/h and 100 km/h respectively. For 64QAM, SNR gain decreases with increasing speed. As before, in the case of an increase in BLER, we observe an increase in SNR gain from 320 km/h to 100 km/h for all types of modulation (QPSK, 16QAM, 64QAM).

Table 2: The OTFS system exhibits superior performance in terms of SNR compared to the OFDM system, as evidenced by BLER values of $2 \cdot 10^{-1}$, $3 \cdot 10^{-1}$, and $6 \cdot 10^{-1}$, respectively.

BLER value	data types	SNR gain for each speed				
		320 kmph	200 kmph	160 kmph	100 kmph	0 kmph
$2 \cdot 10^{-1}$	QPSK	7 dB	6 dB	5.75 dB	5.35 dB	5.25 dB
	16QAM	4 dB	3 dB	2.75 dB	2.25 dB	3 dB
	64QAM	1 dB	2 dB	1.75 dB	1 dB	3 dB
$3 \cdot 10^{-1}$	QPSK	8 dB	7 dB	6.5 dB	6.3 dB	5.25 dB
	16QAM	6 dB	4 dB	3.5 dB	3.25 dB	3 dB
	64QAM	5 dB	1.5 dB	1 dB	0.5 dB	3 dB
$6 \cdot 10^{-1}$	QPSK	9 dB	6 dB	5 dB	4.75 dB	4.5 dB
	16QAM	7.75 dB	4 dB	3.5 dB	3 dB	2.25 dB
	64QAM	5 dB	3 dB	2 dB	1 dB	1 dB

4.2. OTFS and OFDM by a Varying Number of Subcarriers

The following section presents a comparative investigation of the efficiency of OTFS and OFDM modulations. The SNR-based BLER was compared for 128 and 512 subcarriers using QPSK and 16-QAM techniques.

Table 3. The parameters used in the simulation

Parameter	Value
Number of subcarriers	128; 512
Carrier frequency (GHz)	2
speed in kmph	320
Subcarrier spacing (KHz)	15
Cyclic Prefix duration (us)	0.67
Channel model	TDLA
MCS	QPSK, 16QAM, rate 0.5

In Figures 9(a) and 9(b), we plot the BLER versus SNR curves for the two modulation schemes OTFS and OFDM in the case of two different numbers of subcarriers 128 and 512 with a vehicle speed of 320km/h for QPSK and 16QAM.

The two figures, demonstrate the BLER of OFDM to be superior to that of OTFS with a subcarrier number of 128 compared to 512. It can be said that the performance improvement is very small when the SNR increases to 128. At SNR higher than this, the BLER of OTFS becomes lower than that of OFDM.

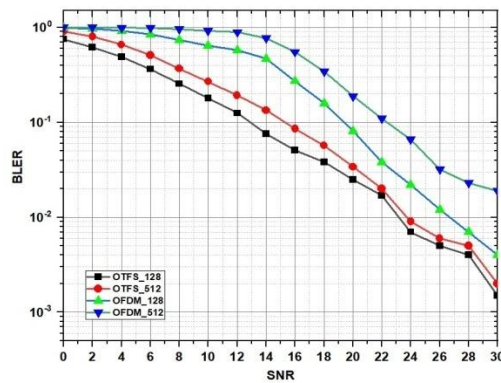


Figure 9 (a): QPSK

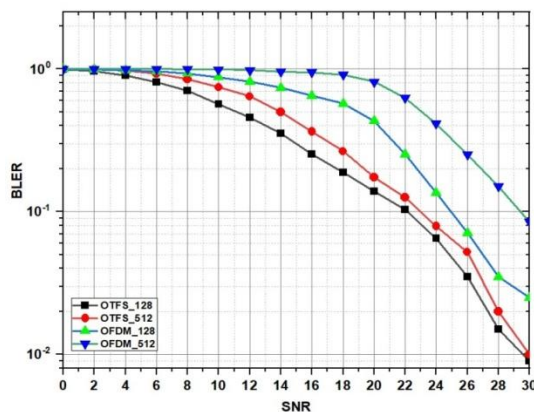


Figure 9 (b): 16QAM

Figure 9: BLER Vs SNR for OFDM and OTFS (15 kHz number of subcarriers M=128 and 512, velocity 320Kmph) with QPSK 16QAM.

5. CONCLUSION

This paper presents an in-depth analysis of Orthogonal Time Frequency Space (OTFS) modulation, comparing it with Orthogonal Frequency Division Multiplexing (OFDM) to evaluate its suitability for 6G wireless networks. By leveraging the delay-Doppler domain, OTFS effectively transforms time-varying channels into quasi-static representations, significantly enhancing resilience to Doppler effects and ensuring superior Block Error Rate (BLER) performance in high-mobility scenarios. Simulations conducted across different mobility speeds, modulation schemes (QPSK, 16QAM, 64QAM), and subcarrier configurations confirm that OTFS maintains robust signal reliability even under severe channel conditions, making it a strong candidate for ultra-reliable low-latency communication (URLLC) and massive IoT applications. Its ability to sustain performance regardless of noise further reinforces its potential in high-mobility and interference-prone environments. However, to enable real-world deployment, future research will focus on optimizing computational complexity, improving channel estimation using machine learning, and integrating OTFS with advanced 6G technologies such as massive MIMO and reconfigurable intelligent surfaces (RIS). Additionally, real-world validation through hardware implementations will be explored to assess its feasibility in high-speed networks. Future work will also investigate fuzzy logic-based channel estimation techniques to further enhance OTFS adaptability in dynamic environments, strengthening its position as a next-generation modulation scheme for 6G communications.

CONFLICTS OF INTEREST

The authors declare no conflict of interest.

REFERENCES

- [1] Paulo Sergio Rufino Henrique; Ramjee Prasad, "6G The Road to the Future Wireless Technologies 2030," in 6G The Road to the Future Wireless Technologies 2030 , River Publishers, 2021, pp.i-xxvi.
- [2] S. Gupta, M. R. Bhatnagar, and R. S. Kshetrimayum, "OTFS Modulation: Performance Analysis and Applications in 5G and Beyond," in *Proceedings of the 2023 IEEE Global Communications Conference (GLOBECOM)*, 2023.
- [3] G. K. Pandey, D. S. Gurjar, H. H. Nguyen and S. Yadav, "Security Threats and Mitigation Techniques in UAV Communications: A Comprehensive Survey," in *IEEE Access*, vol. 10, pp. 112858-112897, 2022, doi: 10.1109/ACCESS.2022.3215975.
- [4] Q. Li, J. Yuan, M. Qiu, S. Li and Y. Xie, "Low Complexity Turbo SIC-MMSE Detection for Orthogonal Time Frequency Space Modulation," in *IEEE Transactions on Communications*, vol. 72, no. 6, pp. 3169-3183, June 2024, doi: 10.1109/TCOMM.2024.3357431.
- [5] DARGHOUTH, Amina, KHLIFI, Abdelhakim, et CHIBANI, Belgacem. "Real time parameter estimation for adaptive OFDM/OTFS selection". *International Journal of Computer Networks & Communications (IJCNC) Vol.16, No.4, July 2024 DOI: 10.5121/ijcnc.2024.16406*
- [6] Li, "Orthogonal Time Frequency Space (OTFS) Modulation for Wireless Communications," Aug. 2022, [Online]. Available: <http://arxiv.org/abs/2208.11807>M. Young, *The Technical Writer's Handbook*. Mill Valley, CA: University Science, 1989
- [7] G. D. Surabhi, M. K. Ramachandran and A. Chockalingam, "OTFS Modulation with Phase Noise in mmWave Communications," 2019 IEEE 89th Vehicular Technology Conference (VTC2019-Spring), Kuala Lumpur, Malaysia, 2019, pp. 1-5, doi: 10.1109/VTCSpring.2019.8746382.
- [8] A. Correas-Serrano, N. Petrov, M. Gonzalez-Huici and A. Yarovoy, "Optimized Time-Frequency Allocation in MIMO NU-OTFS Radar for Enhanced Performance Under Spectral Constraints," 2024 IEEE Radar Conference (RadarConf24), Denver, CO, USA, 2024, pp. 1-6, doi: 10.1109/RadarConf2458775.2024.10548185

- [9] Mounika Siluveru, et al. "Study and Analysis of OTFS and OFDM". Journal of Artificial Intelligence, Machine Learning and Neural Network, vol. 2, no. 06, Nov. 2022, pp. 13-23, doi:10.55529/jaiml.26.13.23.
- [10] M. Sheikh-Hosseini, F. Rahdari, H. Ghasemnezhad, S. Ahmadi and M. Uysal, "A Comparative Performance Evaluation of OFDM, GFDM, and OTFS in Impulsive Noise Channels," in *IEEE Open Journal of the Communications Society*, doi: 10.1109/OJCOMS.2024.3506723
- [11] Vamsi, T. S., Mohanty, H. C., Terlapu, S. K., & Krishna, M. V. (2024). Enhancing 5G Cellular Communications: A Comparative Analysis of OTFS and GFDM Multiple Access Schemes. *International Journal of Multiphysics*, 18(3).
- [12] Fish, Alexander, et al. "Delay-Doppler channel estimation in almost linear complexity." *IEEE Transactions on Information Theory* 59.11 (2013): 7632-7644.
- [13] Li, Shuangyang, et al. "Fundamentals of Delay-Doppler Communications: Practical Implementation and Extensions to OTFS." arXiv preprint arXiv:2403.14192 (2024).
- [14] Yuan, Weijie, et al. "From OTFS to DD-ISAC: Integrating sensing and communications in the delay doppler domain." *IEEE Wireless Communications* (2024).
- [15] Khuc, Bang, et al. "Channel Estimation and Equalization for OTFS Systems Over High-Mobility Channels." 2023 International Conference on Electrical Engineering and Photonics (EExPolytech). IEEE, 2023.
- [16] Mohammed, Saif Khan, et al. "OTFS—A mathematical foundation for communication and radar sensing in the delay-Doppler domain." *IEEE BITS the Information Theory Magazine* 2.2 (2022): 36-55.
- [17] Li, Hua, et al. "OTFS-PDMA Scheme with EPA-Based Receivers for High-Mobility IoT Networks." *IEEE Transactions on Wireless Communications* (2023).
- [18] Chen, Yuhua, et al. "OTFS waveform based on 3-D signal constellation for time-variant channels." *IEEE Communications Letters* 27.8 (2023): 1999-2003.
- [19] Balan, Shanmugha, and Sandeep Joshi. "A Study of High-Speed Railway Communication Channel Models for OTFS-Based Systems." 2024 16th International Conference on Communication Systems & Networks (COMSNETS). IEEE, 2024.
- [20] Shan, Yaru, and Fanggang Wang. "Low-complexity and low-overhead receiver for OTFS via large-scale antenna array." *IEEE transactions on vehicular technology* 70.6 (2021): 5703-5718.
- [21] Ahmed, I. Zakir, and Hamid Sadjadpour. "An ML-assisted OTFS vs. OFDM adaptable modem." 2023 IEEE Future Networks World Forum (FNWF). IEEE, 2023.
- [22] Suvra Sekhar Das; Ramjee Prasad, "OTFS: Orthogonal Time Frequency Space Modulation A Waveform for 6G," in *OTFS: Orthogonal Time Frequency Space Modulation A Waveform for 6G*, River Publishers, 2021, pp.i-xxvi.
- [23] W. Shen, L. Dai, J. An, P. Fan and R. W. Heath, "Channel Estimation for Orthogonal Time Frequency Space (OTFS) Massive MIMO," in *IEEE Transactions on Signal Processing*, vol. 67, no. 16, pp. 4204-4217, 15 Aug.15, 2019, doi: 10.1109/TSP.2019.2919411.
- [24] A. Khan and S. K. Mohammed, "A Low-Complexity OTFS Channel Estimation Method for Fractional Delay-Doppler Scenarios," in *IEEE Wireless Communications Letters*, vol. 12, no. 9, pp. 1484-1488, Sept. 2023, doi: 10.1109/LWC.2023.3274936.
- [25] V. Khammammetti and S. K. Mohammed, "Spectral Efficiency of OTFS Based Orthogonal Multiple Access with Rectangular Pulses," in *IEEE Transactions on Vehicular Technology*, vol. 71, no. 12, pp. 12989-13006, Dec. 2022, doi: 10.1109/TVT.2022.3199478.
- [26] K. Pathak, V. Khammammetti and S. K. Mohammed, "Spectral Efficiency Performance of OTFS Based Multi-Cell Systems," 2023 International Symposium on Networks, Computers and Communications (ISNCC), Doha, Qatar, 2023, pp. 1-6, doi: 10.1109/ISNCC58260.2023.10323654.
- [27] Hadani R, Rakib SS, Monk A, Tsatsanis M, Hebron Y (2020) Orthogonal time frequency space modulation techniques. Patent Application, US20200259692A1, Cohere Technologies, Los Angeles, CA, USA
- [28] P. Ren, B. Cao, Z. Xiang, L. Yang, B. Xu and Y. Li, "OTFS-Based Downlink Network-Coded Multiple Access With Joint Amplitude-Phase Design," in *IEEE Wireless Communications Letters*, vol. 13, no. 6, pp. 1576-1580, June 2024, doi: 10.1109/LWC.2024.3382152.
- [29] P. Priya, E. Viterbo and Y. Hong, "Low Complexity MRC Detection for OTFS Receiver With Oversampling," in *IEEE Transactions on Wireless Communications*, vol. 23, no. 2, pp. 1459-1473, Feb. 2024, doi: 10.1109/TWC.2023.3289610.

- [30] R. Hadani et al., "Orthogonal Time Frequency Space Modulation", 2017 IEEE Wireless Communications and Networking Conference (WCNC), San Francisco, CA, USA, 2017, pp. 1-6, doi: 10.1109/WCNC.2017.7925924
- [31] R. Hadani, S. Rakib, M. Tsatsanis, et al., "Orthogonal Time Frequency Space Modulation," IEEE Transactions on Wireless Communications, vol. 67, no. 9, pp. 6348-6361, 2018.
- [32] T. Datta, N. K. J. Kulkarni, and S. C. S. P. R. Kumar, "Performance of OTFS in Delay-Doppler Channels," IEEE Transactions on Wireless Communications, vol. 68, no. 6, pp. 4400-4416, 2020.
- [33] J. C. O. Nielsen, "Channel Estimation for OTFS Systems," IEEE Communications Letters, vol. 25, no. 3, pp. 567-570, 2021.
- [34] M. K. Sharma and S. Bhattacharjee, "Least Squares and MMSE-based OTFS Channel Estimation," IEEE Transactions on Vehicular Technology, vol. 69, no. 2, pp. 1345-1358, 2020.
- [35] J. Zhang, L. Wu, and P. Fan, "Channel Estimation in OTFS using MMSE Techniques," IEEE Transactions on Communications, vol. 69, no. 1, pp. 234-245, 2021.
- [36] M. D. Renzo, "OTFS for 6G: A Paradigm Shift in Wireless Communications," *IEEE Signal Processing Magazine*, vol. 38, no. 3, pp. 78-94, 2021.
- [37] A. Farhang, M. F. P. Fernandes, and R. R. Maciel, "Message Passing Algorithm for OTFS Detection," *IEEE Transactions on Wireless Communications*, vol. 71, no. 1, pp. 125-138, 2023.
- [38] B. V. S. Reddy, C. Velampalli and S. S. Das, "Performance Analysis of Multi-User OTFS, OTSM, and Single Carrier in Uplink," in *IEEE Transactions on Communications*, vol. 72, no. 3, pp. 1428-1443, March 2024, doi: 10.1109/TCOMM.2023.3332865.

ACKNOWLEDGEMENTS

The authors would like to thank everyone, who has helped and supported this work.

AUTHORS

Abderrahim MOHAMMADI was born in August 1977, in Settat, Morocco. He enrolled in 2021 to prepare the doctorate in the Laboratory of Innovative Systems Engineering at the National School of Applied Sciences of Tetouan, Abdelmalek Essaâdi University, Morocco. His research areas are: Telecommunications systems, Mobile Networks, Cognitive Radio,



Aziz Dkiouak Professor and Researcher at Chouaib Doukkali University, El Jadida. He was born in September 1985, in Tayjoute town, 30 Km from Chefchaouen, Morocco. He received the PhD degree in Electronics and Telecommunications at the Faculty of Sciences, Abdelmalek Essaadi University, Tetuan, Morocco in 2020. His research interests focus mainly on printed microwave circuits and Telecommunications systems. He has authored and co-authored several papers in international refereed journals and conferences in the field of antenna and telecommunications.



Mostafa Baghour was born in Tangier, Morocco. He's a member in the Complex Cyber Physical Systems Laboratory (LCCPS), ENSAM of Casablanca, Hassan II University, Casablanca, Morocco. He's an associate member in the Information and Communication Technology Laboratory (LabTIC), ENSA of Tangier, University of Abdelmalek Essaâdi, Morocco. His research areas are: Wireless Sensor Network, Telecommunications systems, Mobile Networks, Cognitive Radio, Automation, detection and diagnosis systems using signal processing methods. In 2002, he obtained the master's degree in electrical and computer engineering from the Faculty of Sciences and Techniques of Tangier, Morocco. He continued his studies to obtain the ENS of Rabat diploma in the computer science specialty in 2004. In 2006, he received DESA diploma in Automatics and information processing at the FST of Tangier. Thereafter, He obtained the doctorate degree in Physics and Embedded System. He has taught at several educational institutions. Currently, he is an assistant



professor at the department of Electrical Engineering at ENSAM of Casablanca, Hassan II University, Morocco.

Saad Chakkor was born in Tangier, Morocco. He's a member in the Information and Communication Technology Laboratory (LabTIC), National School of Applied Sciences in Tangier, University of Abdelmalek Essaâdi, Morocco. His research areas are: Telecommunications systems, Mobile Networks, Cognitive Radio, Wireless intelligent Sensors Networks and theirs applications, frequency estimation algorithms, Automation, detection and diagnosis systems using signal processing methods. In 2002, he obtained the Maîtrise's degree in Electrical and Computer Engineering from the Faculty of Sciences and Techniques of Tangier, Morocco. He continued his studies to obtain the ENS of Rabat diploma in the computer science specialty in 2003. In 2006, he received DESA diploma in Automatics and information processing at the FST of Tangier. Thereafter, He obtained the doctorate degree in Automatics and Telecommunications from the Faculty of Sciences of Tetouan in 2015. He has taught at several educational institutions. Currently, he works teacher of Telecommunications in the ENSAT School.



Ahmed El Oualkadi received his Ph.D. in electrical engineering from the University of Poitiers, France, in 2004. He has held academic and research positions in France and Belgium, focusing on RF circuit design, low-power systems, and wireless communication technologies. Currently, he is a full professor and deputy director at National School of Applied Sciences of Tetouan, Abdelmalek Essaadi University, Morocco. He has supervised numerous theses, authored over 80 publications, edited 5 books, contributed to 14 book chapters, and holds a patent. He is an active member of IEEE, EuMA, and several scientific committees, and has organized multiple international conferences. His research interests include electronics, RFIC design and ICT.



Anass El Mamouni, PhD, Professor and Researcher at Abdelmalek Essaadi University. He was born in Tangier, Morocco. He earned a Master's Degree in Applied Higher Studies (DESA) in Materials Physics in 2000 and completed his PhD in Materials Science at the Faculty of Science and Technology of Tangier in 2019. Since 2020, he has been a professor at the National School of Applied Sciences of Tangier (ENSAT) within the Department of Information and Communication Systems. Prior to this, he taught for several years as a senior lecturer in the preparatory classes for engineering schools in Morocco. He is an active member of the Laboratory of Communication and Information Technologies (LabTIC), where his research focuses on materials, antennas, and microwave technologies. He has published several papers in these fields and contributes to advancing research in wireless communication technologies.

